ELSEVIER

Agricultural and Forest Meteorology 80 (1996) 135–163

AGRICULTURAL AND FOREST METEOROLOGY

Optically-based methods for measuring seasonal variation of leaf area index in boreal conifer stands

Jing M. Chen *

Canada Centre for Remote Sensing, #419-588 Booth Street, Ottawa, Ont. K1A 0Y7, Canada

Received 27 February 1995; accepted 25 July 1995

Abstract

The feasibility of detecting the seasonal variation in leaf area index (LAI) in boreal conifer forests is investigated using optical instruments. The LAI of six stands was measured. They include young and old jack pine (*Pinus banksiana*) and old black spruce (*Picea mariana*) located near the southern border (near Prince Albert, Saskatchewan) and near the northern border (near Thompson, Manitoba) of the Canadian boreal ecotone. LAI values of the stands are obtained by making several corrections to the effective LAI measured from the LI-COR LAI-2000 Plant Canopy Analyzer (PCA). The corrections include a foliage element (shoot) clumping index (for clumping at scales larger than the shoot) measured using the optical instrument TRAC (Tracing Radiation and Architecture of Canopies) developed by Chen and Cihlar (Chen, J.M. and Cihlar, J., 1995a, Plant canopy gap size analysis theory for improving optical measurements of leaf area index of plant canopies, Appl. Opt., 34: 6211–6222), a needle-to-shoot area ratio (for clumping within the shoot) obtained from shoot samples, and a woody-to-total area ratio obtained through destructive sampling of trees. It is found that the effective LAI varied about 5% to 10% in the growing season and the element clumping index remained almost unchanged. The needle-to-shoot area ratio varied the most, about 15% to 25%, which is of the same order of magnitude as the expected seasonal variability in LAI. This demonstrates that most of the seasonal variation information is contained in the needle-to-shoot area ratio, which can not be measured indirectly using in situ optical instruments and has to be obtained from a large quantity of shoot sample analysis which is laborious and error-prone. Based on our experience, an improved and convenient shoot sampling strategy is suggested for future studies. The optically-based LAI values were compared with destructive sampling results for three of the stands. Based on error analysis, we believe that optical measurements combined with shoot sample analysis can produce LAI values for conifer stands which are more accurate than destructive sampling results.

* Corresponding author.

SSDI 0168-1923(95)02291-0

1. Introduction

Although conifer forests are ever green, they also undergo the annual cycles of new growth in the spring and senescence in the fall. Their leaf area index (LAI), defined as half the needle surface area per unit ground surface area (Chen and Black, 1992b), is therefore variable during the course of a year. In satellite remote sensing, vegetation indices, calculated using the reflectance in red and near infrared wavebands, show large seasonal variations with maxima in the summer and minima in the winter for conifer forests (Cihlar, 1996). The variations are caused by several factors including LAI of the understory and overstory, chlorophyll content in leaves, snow cover, soil type, and others. Because of the effects of these factors, large uncertainties exist in the algorithms for deriving LAI of conifer stands from satellite data (Spanner et al., 1990; Chen and Cihlar, 1996). To improve the algorithms, quantitative information on the seasonal variation in the overstory LAI is critical. Such information is also important for modelling carbon budget of the forests (Bonan, 1993; Running and Hunt, 1992) and the interaction between vegetation and the atmosphere (Sellers et al., 1986).

The seasonal variability in LAI depends on the average life span of green needles and the amount of new growth in the current and previous years. Since boreal conifer trees generally carry needles for any given year for up to four to ten years, the seasonal variability is expected to be about 25–30%, which is similar to the uncertainties of many techniques (direct or indirect) for measuring LAI. Therefore, the attempt to measure the seasonal variation in LAI has not previously been made. With the advent of the TRAC (Tracing Radiation and Architecture of Canopies) instrument developed and tested by Chen and Cihlar (1995a, b), much of the uncertainties in the optical measurements of LAI have been reduced, and therefore it may be possible to detect the seasonal variation. The overall goal of this paper is to assess optical techniques for measuring LAI and detecting the seasonal variability.

Chen and Cihlar (1995a) delineated three major issues in optical measurements of LAI:

1. leaf angle distribution,
2. leaf spatial distribution, and
3. the contribution of the supporting woody material to light attenuation.

The first two issues were addressed by them, while the third was not. In this paper, all these three issues are considered and the methodology for each of them is evaluated by comparing measurements made at different times in the growing season. The problem with leaf angle distribution is largely solved with multiangle measurements using Plant Canopy Analyzer (LAI-2000, LI-COR, Lincoln, NE). The effect of non-random spatial distribution of foliage is quantified using a foliage clumping index because needles in conifer canopies are clumped into shoots (a collection of needles), branches and tree crowns. Much research effort is directed towards the effect of foliage clumping on LAI measurements (Smith et al., 1993; Stenberg et al., 1994). In modelling radiation regimes and productivity in conifer stands, the importance of conifer shoot structure has long been recognized and investigated (Norman and Jarvis, 1974; Oker-Blom, 1986; Leverenz and Hinckley, 1990). Ross et al. (1986) provided detailed measurements of Scots pine shoot structure in the attempt to improve canopy modelling. Chen and Black

(1992a, b) and Chen and Cihlar (1995a, b) first provided optical evidence for the treatment of conifer shoots as the basic foliage units (elements). The clumping index is therefore separated into two components:

1. for clumping scales larger than the shoot (quantified using the element clumping index); and
2. for within shoot clumping (quantified using the needle-to-shoot area ratio).

The element clumping index is measured using the TRAC, and the needle-to-shoot area ratio is obtained through laboratory analysis of shoot samples following the methodology of Chen and Black (1992a, b) and Fassnacht et al. (1994). The methodology is different from the previous method of Gower and Norman (1990) and Deblonde et al. (1994). To address the third issue on the contribution of supporting woody material, labour intensive destructive sampling was conducted in three of the six stands. and allometric relationships between tree trunk diameter and the leaf area or woody area were developed for these three stands. The specific objectives of this paper are:

1. to determine which component of the optical measurements or shoot sampling is most affected by the seasonal variation in LAI;
2. to evaluate the feasibility of detecting the seasonal variability using the optically-based methods; and
3. to identify the areas for improvements.

2. Theory

The angular distribution of canopy gap fraction, $P(\theta)$, where θ is the zenith angle, is generally described as follows (Nilson, 1971):

$$P(\theta) = \exp[-G(\theta)\Omega L_t/\cos\theta] \quad (1)$$

where $G(\theta)$ is the projection coefficient, L_t is the plant area index defined as one half the total surface area of leaves and supporting woody materials per unit ground surface area (Chen and Black, 1992b), Ω is the total foliage clumping index. Eq. (1) is derived based on the Markov chain theory to estimate the probability of beam penetration through multiple independent canopy layers. It can be considered as a modified Poisson model to account for the variation in foliage spatial distribution patterns. When $\Omega = 1$, the canopy is random, and Eq. (1) returns to the Poisson model. An alternative to this method is the negative binomial function which characterizes the leaf dispersion with N, the number of independent foliage layers in the canopy (Oker-Blom, 1986; Baldocchi et al., 1985). This alternative suffers from the difficulty in determining the value of N.

Since many optical instruments such as the PCA measure $P(\theta)$, from which only the product of Ω and L_t is obtained, ΩL_t is therefore called the effective LAI denoted as L_e, (Chen et al., 1991). When L_e is measured, L_t can be obtained from

$$L_t = L_e/\Omega. \quad (2)$$

The clumping index, Ω, is therefore a correction factor required to convert L_e to L_t.

Note that the smaller the Ω, the more clumped is the canopy. By treating shoots as the basic foliage units, Chen and Cihlar (1995b) derived that

$$\Omega = \Omega_E / \gamma_E \tag{3}$$

where Ω_E is the element clumping index quantifying the effect of foliage clumping at scales larger than the shoot, and γ_E is the needle-to-shoot area ratio for the foliage clumping within the shoot. By combining Eqs. (2) and (3) we have

$$L_t = L_e \times \gamma_E / \Omega_E . \tag{4}$$

The plant area index L_t is the sum of leaf area index, denoted by L, and the woody area index, denoted by W, and therefore

$$L = L_t - W = L_t(1 - \alpha) \tag{5}$$

where $\alpha = W/L_t$. From Eqs. (4) and (5), the final equation is

$$L = (1 - \alpha) L_e \times \gamma_E / \Omega_E . \tag{6}$$

The above equation shows that to obtain the true leaf area index, three corrections must be made to the effective leaf area index, L_e, obtained from multi-angle gap fraction measurements.

2.1. Effective leaf area index, L_e

Using the formula of Miller (1967), Chen and Black (1991) showed that

$$L_e = 2\int_0^{\frac{\pi}{2}} \kappa(\theta) \sin\theta \, d\theta \tag{7}$$

where $\kappa(\theta)$ is the mean contact number per unit canopy height and is defined as

$$\kappa(\theta) = \cos\theta \ln[1/P(\theta)] . \tag{8}$$

Eqs. (7) and (8) show that to obtain the L_e of a canopy, the gap fraction distribution, $P(\theta)$, is required over the zenith angle range from 0 to $\pi/2$, and the calculated $\kappa(\theta)$ gains an increasing weight as θ increases. However, in practice, the relative measurement error in $P(\theta)$ increases with θ because $P(\theta)$ becomes smaller at larger zenith angles. This inherent problem with optical measurements may be alleviated in the case of conifer stands, given the fact that the basic foliage units, the shoots, are approximately spherical and hence $\kappa(\theta)$ does not change much over the entire incident angle range. For perfect spherical foliage elements, or spherical leaf angle distribution in the case of flat leaves, $\kappa(\theta)$ is a constant, resulting in the projection coefficient, $G(\theta)$, of 0.5.

The PCA measures $\kappa(\theta)$ at discrete θ values of 7°, 23°, 38°, 53° and 68° from which L_e is calculated as the $\sin\theta$ weighted mean of $\kappa(\theta)$ at these five angles.

2.2. Needle-to-shoot area ratio γ_E

Shoots of conifer forests are distinct foliage units. Very often, needles are tightly grouped in shoots, making it impossible to infer the amount of needle surface area from

optical measurements. Recognizing this problem, Gower and Norman (1990) used the ratio of projected needle area to the projected shoot area at one angle as a correction to the PCA measurement to obtain leaf area index. The approach is similar to those by Norman and Jarvis (1974), Oker-Blom (1986) and Leverenz and Hinckley (1990) in studies of radiation in conifer canopies. Chen and Black (1992a) improved the correction methodology by using the ratio of half the total needle area in a shoot (A_n) to half the total shoot area (A_s). Fassnacht et al. (1994) developed an apparatus for measuring A_s and provided a formula for calculating A_s from discrete projections of shoots. By the definition of Chen and Black (1992a) and Chen and Cihlar (1995a),

$$\gamma_E = A_n/A_s \tag{9}$$

and

$$A_s = \frac{1}{\pi}\int_0^{2\pi} d\phi \int_0^{\frac{\pi}{2}} A_p(\theta,\phi)\cos\theta \, d\theta \tag{10}$$

where ϕ is the azimuth angle of the projection relative to the direction of the shoot main axis (in the case of a fixed vertical position for the camera, it is the azimuth angle of the shoot main axis relative to any reference azimuth angle), θ is the angle between the projection and the normal to a surface on which the shoot main axis is rested (in the case of the light table-camera system shown in Fig. 1 of Fassnacht et al. (1994), the surface is the light table), and $A_p(\theta,\phi)$ is the projected area at θ and ϕ. If $A_p(\theta,\phi)$ does not vary with θ and ϕ, A_s equals $2A_p$ (i.e. for projections of a sphere, A_s is the half the sphere surface area). For projections of solids or foliage clumps of other shapes, A_s always equals half the total surface area of the solids or the imaginary surface area of the clumps (Lang, 1991; Chen and Black, 1992b). The imaginary clump surface area is the area enveloping the clump, and Eq. (10) provides an effective way to obtain such an area. We believe that in conifer stands where shoots are dense, it is A_s and not A_n which is responsible for light interception. In other words, optical instruments measure A_s rather than A_n, and Eq. (9) provides a means to obtain the needed quantity A_n from A_s in the same unit.

Eq. (10) in this form appears to be similar to Eq. 9 in Fassnacht et al. (1994) when written in a discrete form but differs in one essential aspect: $\cos\theta$ rather than $\sin\theta$ is used as a weight. In both cases, the meaning of θ is the same: the view zenith angle of the camera (or regarded as the projection angle). The assumption is also the same: shoots are randomly (spherically) distributed with respect to their orientation. The projection of conifer shoots is also approximated using cylinders in both cases. Chen and Black (1992b) demonstrated that when the long axis of cylinders is randomly distributed with respect to its angular position, the projection coefficient becomes a constant of 0.5 irrespective of the angle of projection, suggesting that the assumption of the random distribution of shoot main axis is a good basis for the calculation. The demonstration is shown through the derivation of Eq. 23 in Chen and Black (1992b), where α_L is the inclination angle of the cylinder's long axis (not the angle of projection) and $\sin\alpha_L$ is the weight. In the light table-camera system, θ is zero when the camera is vertical and the light table is horizontal, but in this case, α_L is $\pi/2$ because the shoot main axis is horizontal ($\pi/2$ from the projection direction). By definition, $\alpha_L = (\pi/2) - \theta$, there-

fore $\cos\theta = \sin\alpha_L$. The physics of the weighting scheme is easily understood by imaging a sphere with cylinders inserted uniformly perpendicular to the surface. The projection of the cylinders on a plane perpendicular to the projection direction in this case is independent of the projection direction because of the spherical nature. Whatever the incident direction may be to the sphere, there are always more cylinders perpendicular to the incident light than cylinders parallel to the light, i.e. heavier weights are given to cylinders with smaller θ values (zero means perpendicular to the incident light). This would suggest that $\cos\theta$ is the correct weighting scheme. The physics is perhaps better understood by deriving Eq. 23 from Eq. 22 in Chen and Black (1992b).

In the present study, the same apparatus of Fassnacht et al. (1994) was used for measuring A_s for a sub-sample of shoots. In most cases, the camera incident angles to the light table (θ) were 15°, 45° and 75°, and the azimuth angles were 0°, 15°, 30°, 45°, 60°, 75° and 90°, resulting in 21 projection angles. In some cases, the azimuth angle range was extended to 180° with the same increment, leading to 39 projection angles. The calculated A_s values under these two measurement schemes were nearly identical for the same shoots, suggesting it is unnecessary to measure beyond the 90° azimuth angle range. Because of the large quantity of shoots samples processed in this study, most shoots were measured at only three camera incidence angles: 0°, 45° and 90° at an azimuth angle of 0°. Since the weight of $\cos\theta$ is zero at $\theta = 90°$, the projected area at 90°, A_p (90°, 0°), was treated as that at 75°. To counter balance the bias because of the treatment, the measurement at 0° was used as that at 15°. The differences were small, and it is much easier in practice to measure at 0° and 90° than at 15° and 75°. The simplified equation for calculating A_s becomes

$$A_s = 2\frac{A_p(0°,0°)\times\cos(15°) + A_p(45°,0°)\times\cos(45°) + A_p(90°,0°)\times\cos(75°)}{\cos(15°)+\cos(45°)+\cos(75°)} \tag{11}$$

The results from the three-angle measurement scheme agree very well with the 21- or 39-angle measurement schemes for both jack pine and black spruce species. We recommend this simple method for future studies.

2.3. Element clumping index Ω_E

If shoots are randomly positioned in the canopy, the correction using the needle-to-shoot area ratio is sufficient to obtain the plant area index. However, conifer canopies are always highly organized at several levels: shoots, branches, whirls and tree crowns. Grouping of foliage at these levels results in a canopy gap fraction larger than the case of a random canopy. The element clumping index is used to quantify the effect of clumping at scales larger than the shoot.

For the same canopy gap fraction, defined as the fraction of sky seen from underneath the canopy, there can be different canopy gap size distributions. Gap size refers to the actual physical dimension of a gap. A canopy gap size distribution carries information on the canopy architecture, and therefore can be used to quantify the effect of the architecture on the LAI measurements which are based on the gap fraction

principle. Chen and Black (1992a) used a measured canopy gap size distribution from the transmitted solar beam on a tramway to derive the element clumping index for a Douglas-fir (*Pseudotsuga menziesii*) canopy. They developed a theory based on the assumption that shoots are randomly distributed in tree crowns (clumps) and tree crowns are randomly distributed in space. For the same purpose, Chen and Cihlar (1995a) developed an improved theory without using these assumptions. Chen and Cihlar (1995b) compared these two theories and concluded that the later is more general and accurate, but the former has the merit of being capable of deriving canopy architectural parameters. In this paper, Chen and Cihlar's theory is used for calculating the element clumping index and is outlined as follows.

The TRAC instrument measures the transmitted direct solar irradiance at an interval of about 10 mm along transects beneath the canopy. From the measurements, sunflecks (sunlit patches on the forest floor) of various sizes can be identified. A sunfleck size can be converted into a canopy gap size after considering the penumbra effect. The gaps along the transect can be sorted in descending order according to their size. From the sorted gap size series, a gap size distribution curve $F_m(\lambda)$ can be formed, where $F_m(\lambda)$ is the fraction of gaps larger than or equal to the gap size λ. For a canopy with a random spatial distribution of foliage elements, the gap accumulation curve denoted by $F(\lambda)$ is predicted by (Miller and Norman, 1971)

$$F(\lambda) = \left(1 + L_p \frac{\lambda}{W_{E_p}}\right) e^{-L_p(1+(\lambda/W_{E_p}))} \tag{12}$$

where

$$L_p = \frac{G(\theta) L_E}{\cos\theta} \tag{13}$$

In the above equations, L_E is the element (shoot) area index defined as half the total shoot area (A_s) per unit ground surface area, W_{E_p} is the mean projected width of shoots along the direction of the transect. These are the only two parameters controlling the gap size distribution in the canopy. When the canopy is not random, the measured distribution curve $F_m(\lambda)$ deviates from $F(\lambda)$. If the canopy is clumped with respect to tree crowns and branches, the probability of seeing large gaps dramatically increased from the predictions for random canopies. The excessively large gaps can therefore be identified by comparing $F_m(\lambda)$ with $F(\lambda)$, and the contributions of the large gaps due to clumping can be removed from the gap accumulation. After the removal of all gaps in excess of $F(\lambda)$, the canopy is compacted and becomes pseudo random. The measured total canopy gap fraction is then reduced from $F_m(0)$ to $F_{mr}(0)$, where $F_{mr}(\lambda)$ is $F_m(\lambda)$ brought to the closest agreement with $F(\lambda)$ through the gap removal procedure. The element clumping index is then calculated as

$$\Omega_E = \frac{(1 + \Delta g)\ln[F_m(0)]}{\ln[F_{mr}(0)]} \tag{14}$$

where Δg is the total gap fraction removed and is $F_m(0) - F_{mr}(0)$.

In the gap removal procedure, $F(\lambda)$ is calculated first. The calculation requires both W_{E_p} and L_p. While W_{E_p} can be obtained from shoot analysis, L_p is unknown. Chen and

Table 1
Stand description

Stand	Age (year)	Tree height (m)	Density (stems/ha)	Latitude (deg)	Longitude (deg)	Transect length (m)
SOJP	60–75	12–15	1600–2400	53.916 N	104.692 W	200
SYJP	11–16	4–5	4000–4100	53.877 N	104.647 W	300
SOBS	0–155	0–11	3700–4400	53.987 N	105.122 W	300
NOJP	50–65	9–13.5	1300–2600	55.928 N	98.624 W	210
NYJP	25	0–2.5	5700–42000	55.905 N	98.288 W	340
NOBS	75–90	9–12	1150–8700	55.880 N	98.484 W	300

Cihlar (1995a) developed an iteration procedure which avoids the prior knowledge of L_p. In the iteration, L_p is equal to $-\ln[F_{mr}(0)]$, where $F_{mr}(0)$ is first taken as $F_m(0)$, and a precursory $F(\lambda)$ is calculated as the first basis for gap removal. As the largest gaps are removed, $F_{mr}(0)$ decreases and L_p increases. The iteration proceeds by refining L_p and ceases when L_p reaches an asymptotic value or when part of $F_{mr}(\lambda)$ becomes smaller than $F(\lambda)$.

3. Experimental methods

The investigation presented in this paper is part of the Boreal Ecosystem-Atmosphere Study (BOREAS). Optical and destructive measurements of LAI were made in conifer stands in the Southern Study Area (SSA) near Candle Lake, Saskatchewan, and in the Northern Study Area (NSA) near Thompson, Manitoba, during BOREAS intensive field campaigns in 1993 and 1994. The stand attributes are summarized in Table 1, where SOJP, SYJP and SOBS are old jack pine (*pinus banksiana*), young jack pine and old black spruce (*Picea mariana*), respectively, in the SSA, and likewise NOJP, NYJP and NOBS in the NSA.

These stands were within the BOREAS tower flux sites. They were reasonably homogeneous at scales up to 1 km. Three transects were established in each stand. The lengths of the transects are specified in Table 1. The transects in each stand were parallel and separated by 10 m. In SOBS, SOJP, NOBS and NOJP, the middle transect of the three, marked A, B and C, started from the main flux tower and extended towards the southeast, but in SYJP and NYJP, the middle transect was centred at the tower and ran in both the southeast and northwest directions.

3.1. Optical measurements

Optical instruments were used to measure LAI along the transects in the following BOREAS intensive field campaigns: IFC-93 (9 August to 29 August 1993); IFC-1 (5 May to 16 June 1994); IFC-2 (19 July to 8 August 1994) and IFC-3 (30 August to 19 September). The instruments used were the PCA (LAI-2000, LI-COR, Lincoln, NE) and the TRAC. The PCA measures diffuse blue light (400–490 nm) from the sky simultane-

ously in five equal zenith angle ranges from 0 to 75°. It is assumed in the PCA that foliage is black and scattering of blue light in the stand is negligible. To minimize the scattering effect, all PCA measurements were made under no or very small direct light conditions. This was achieved by taking the measurements near sunset or under overcast conditions. PCA measurements were made along the transects at a 10 m interval at fixed locations marked with forestry flags. For each stand, the data were acquired at about 90 locations each time. Most of the time, three PCA units were used. One was mounted either on the top of the flux tower or in a nearby clearing to obtain the above-stand reference readings. Precautions were taken in placing the reference PCA to ensure that no objects significantly obstruct the sky view above 15° elevation angle. The reference readings were taken in remote mode every 15 sec. The other two units were used by two persons walking on the transects simultaneously. Usually 90 readings were made within 20 min. The three units were synchronized regularly (every 10 days) and calibrated once in IFC-93 and twice during the summer 1994 following the procedures recommended in Appendix C of the Instruction Manual of the PCA. The 90° view caps were used for all three units all the time to block the bright sky near the sun's direction and to eliminate the shadowing effect of instrument operators. During measurements, the operator stood between the sensor and the sun. The in-stand and reference measurements were merged together later using the PCA program c2000.exe to calculate the effective LAI. In the calculation, the option 'ACT' was selected to match pairs of 'A' (above stand) and 'B' (in stand) readings closest in time, and no ring masks were used in the computation.

An investigation on the scattering effect was carried out by masking rings four and five (near horizontal) in the calculation. The LAI results in jack pine stands with these two rings removed were about 5% smaller that those calculated with five full rings. The results contradict the general case where removal of the outer rings results in larger LAI values because the scattering contamination of the data is most serious at larger zenith angles. The reason for the contradiction is either because the scattering effect is small in the open stands or the effect is overly compensated by erectophile foliage distributions. An erectophile canopy allows more light penetration per unit pathlength through the canopy in near vertical directions than in near horizontal directions, and, therefore, removing the rings near the horizontal direction results in smaller LAI values. The inclination angle distribution of the shoot main axis was measured in SOBS, SYJP and NYJP stands using a simple device consisting of a protractor and a string. In both SYJP and NYJP, there were more shoots with the main axis near the vertical position than near the horizontal position, showing erectophile distributions. In the SOBS stand, the opposite was found, i.e. the distribution was planophile. However, the shoot angle distribution is only part of the foliage angle distribution because the shape of tree crowns is also important in determining the light penetration at different incident angles. In the SOBS stand, the large part of the tree crowns are of cylindrical shape with a height-to-diameter ratio of about one to five. Since a canopy consisting of vertical cylinders is erectophile, the tree crown structure tends to make the SOBS stand erectophile, counter-acting the effect of shoot angle distribution. Because the foliage angle distribution deviates considerably from random conditions, the scattering effect can not be quantified using the PCA data alone, and thus it is not justified to exclude the outer rings in the LAI calculation.

On the same transects, the TRAC was used on cloudless days. The new version of the TRAC used in 1994 consists of three quantum sensors (LI-COR, Lincoln, NE, Model LI-190SB, 10 μs time constant), a data logger (Campbell Scientific, Logan, UT, Model CR10) and a storage Module (Model SM716). Two of the sensors faced upwards to measure the downwelling total and diffuse PAR, and one faced downward to measure the reflected PAR from the forest floor. For the diffuse sensor, a vertical shading strip was used on the side to obstruct the direct light. The sensors were supported by a holding arm and connected to the data logger operated at a sampling frequency of 32 Hz. The whole system was hand-carried by a person walking along pre-established transects. With a walking pace of 1 m per three seconds, a sampling interval of 10 mm for each sensor could be achieved. During measurements, the operator needed to control the pacing while watching a leveling bubble and the shading to the diffuse sensor simultaneously. At each flag separated by 10 m along the transects, a button on the holding arm was pressed to register the distance on the data logger and a measurement spatial interval for each 10 m was calculated assuming a constant walking speed within the interval. The TRAC was used in this study by several operators at different times. They were all able to pace within 10% of the required speed. The sensors were carried at approximately 0.6 m above the forest floor in tall stands (SOBS, SOJP, NOBS and NOJP) and 0.1–0.2 m in short stands (SYJP and NYJP). For LAI calculations, only the two upward facing sensors were used. Canopy gap fraction and gas size were calculated using the transmitted direct irradiance taken as the difference between the output of the two sensors. The diffuse irradiance varied the most in NYJP (about 25% in 10 m) and the least in SOJP (about 3% in 10 m). Calculating the direct PAR using two sensors is a significant improvement over the calculation using one sensor (Chen and Cihlar, 1995a, b, 1996). Frequently, the shading strip failed to obstruct the direct sunlight to the diffuse sensor and sharp spikes appear in the diffuse irradiance time trace. A program was written to remove the spikes and to replace them with the mean values of 50 adjacent unaffected readings. The procedures developed by Chen and Black (1992a, b) and refined by Chen and Cihlar (1995a, b) were used to isolate each sunfleck and compute the corresponding canopy gap size from the direct irradiance trace.

3.2. Shoot analysis

In order to obtain the within-shoot clumping factor as one of the corrections to the PCA measurements, shoot samples were taken from each of the stands in IFC-1, IFC-2 and IFC-3. To obtain an average value for a stand, trees were first grouped into three categories by their height and size: dominant (D), co-dominant (M) and suppressed (S), and one tree was selected from each class for shoot samples. From each tree, shoot samples were taken at three heights: top (T), middle (M) and low (L), thus creating nine shoot classes: DT, DM, DL, MT, MM, ML, ST, SM and ST, for each stand. In IFC-1, three shoots were sampled from each class, creating a total of 27 shoots per stand, but in IFC-2 and IFC-3, samples were increased to 5 to 10 per class.

Shoot samples were analyzed in the laboratory for the needle-to-shoot area ratio and the average shoot width used as the element width for TRAC data analysis. For measuring the shoot projected area required in Eq. (12), a video camera-computer

system (AgVision, Decagon Devices Inc., Pullman, WA) was used. The system was calibrated using opaque paper strips of similar size to the needles to minimize the edge effect and to find the threshold value. The calibration was checked every time the system was moved between the SSA and NSA some 750 km apart. The threshold value varied between 168 to 173. The variation may be due to different room lighting conditions. We found that the system was reliable for measuring large objects like shoots but inadequate for measuring small objects like black spruce needles. To measure needle area accurately, a volume displacement method was used. The method is described by John Norman in Appendix K in BOREAS Experimental Plan (Version 3.0). Briefly, to know the total needle area in a shoot, the whole shoot with the stem is immersed in water in a container resting on a sensitive balance (0.01 g). The displaced water volume is measured as the increase in weight if the shoot is not touching the side or the bottom of the container because the displaced water exerts forces equally in all directions including the bottom of the container. To obtain the displaced volume of needle only, the total volume is reduced by the stem volume measured in the same way with needles removed. The equations used for calculating half the total needle area A (in cm^2) are

$$A = 2.05\sqrt{V \times n \times l} \quad \text{for jack pine} \tag{15}$$

$$A = 2.00\sqrt{V \times n \times l} \quad \text{for black spruce} \tag{16}$$

where V is the displaced volume (cm^3 or g) of the needles in a shoot, n is the total number of needles submerged and l is the average length (in cm). The procedure for the shoot analysis includes the following steps:

1. measuring the projected shoot area in 3 (or 21 or 39) angular positions;
2. immersing the shoot and reading the displaced volume from the weight increase;
3. cutting off the needles from the stem and immersing the bare stem to obtain the displaced volume by the stem;
4. counting the number of needles from the shoot and measuring the average length of needles.

There were usually about 100 to 200 needles in a shoot, and thus the length of the needles was obtained from a randomly selected sub-sample of 20 needles. The selected needles were lined up and the total length was measured. The total shoot area was calculated using the projected area at the three angles using the simplified formula (Eq. (11)). Half the total needle area in a shoot was calculated using Eqs. (15) and (16).

Because a large number of shoots was required to characterize a stand, only a sub-sample of shoots (11 from each of NOBS, NYJP and SOJP, and 10 from NOJP) were subjected to a complete analysis for their angular projection behaviour. Projected area was measured at 21 angles for all shoots in the sub-samples and at 39 angles for eight shoots (two from each sub-sampled stands). The exact 21 and 39 angles are described in Section 2 (Theory). The 39 angles were used to ensure that asymmetry of needle distribution around the stem does not cause a significant difference in the weighted projected area using Eq. (11). Because needles were reasonably evenly distributed around the stem for both jack pine and black spruce species, the difference was found to be negligibly small. When three-angle results are plotted against 21-angle

results, almost perfect one-to-one lines are found with less than 2% deviation from the line for NOBS, NOJP and NYJP and less than 5% for SOJP.

3.3. Destructive sampling of LAI and WAI

Three to four trees were felled in NOJP, SOJP and SOBS stands in IFC-3 to assess LAI and woody area index (WAI) of the stands and to use them for validation of the indirect measurements with optical instruments. Tree trunk diameter at the breast height (D_{bh}) were first measured in a 20 m by 100 m area in NOJP and SOJP and in a 20 m by 50 m area in SOBS. The trees measured were grouped into four categories according to their diameter: dominant (D), co-dominant (M), suppressed (S), and new growth (N). The new growth category is only found in SOBS.

One tree was selected from each category. The tree crown was separated into three height classes: T, M and L, similar to the classification for shoot sampling. To obtain the needle area of the whole tree, all shoots were clipped and bagged by class to obtain the fresh weight immediately in laboratory. Five shoots were randomly selected from each class as a sub-sample to obtain the ratio of needle area to fresh weight. The needle area of the sub-sampled shoots was measured using the volume displacement method described above. The ratio is then used to convert the fresh weight of the whole bag into needle area. Care was taken in clipping the shoots to allow only a 10 mm stem lead at each shoot base which was needed for the shoot immersion.

After all the shoots were clipped, the area of the branches was measured. To reduce the work load, similar adjacent branches were grouped and one representative branch for the group (two to 10 branches) was measured in detail. The measurements on a representative branch include branch base and tip diameters, main branch length, the number of secondary branches, base and tip diameters and length of one or two representative secondary branches, the number of end branches (without further divisions), the base diameter and the length of one or two representative end branches. In this way, all branches, live or dead, on the tree were measured.

4. Results and Discussion

4.1. Effective leaf area index

Fig. 1(a)–(f) shows the spatial variation in the effective LAI as directly measured by the PCA for SOBS, NOBS, SOJP, NOJP, SYJP and NYJP, respectively. (The discontinuity of data near the tower is due to limited access to the protected instrumental area.) Even though all the tower flux sites were carefully selected for homogeneity, there were small and large scale variations in the density of the forest cover represented by the effective LAI. Large scale variations were more apparent in both NOBS and SOBS stands, where clear trends of decrease or increase in the effective LAI are easily detectable at 50 m to 100 m scales. The small scale variations were most pronounced in NYJP and SYJP. SOJP was the most uniform stand at all scales. In NOJP, there were many sharp spikes in the L_e distribution. These measurements were affected by the

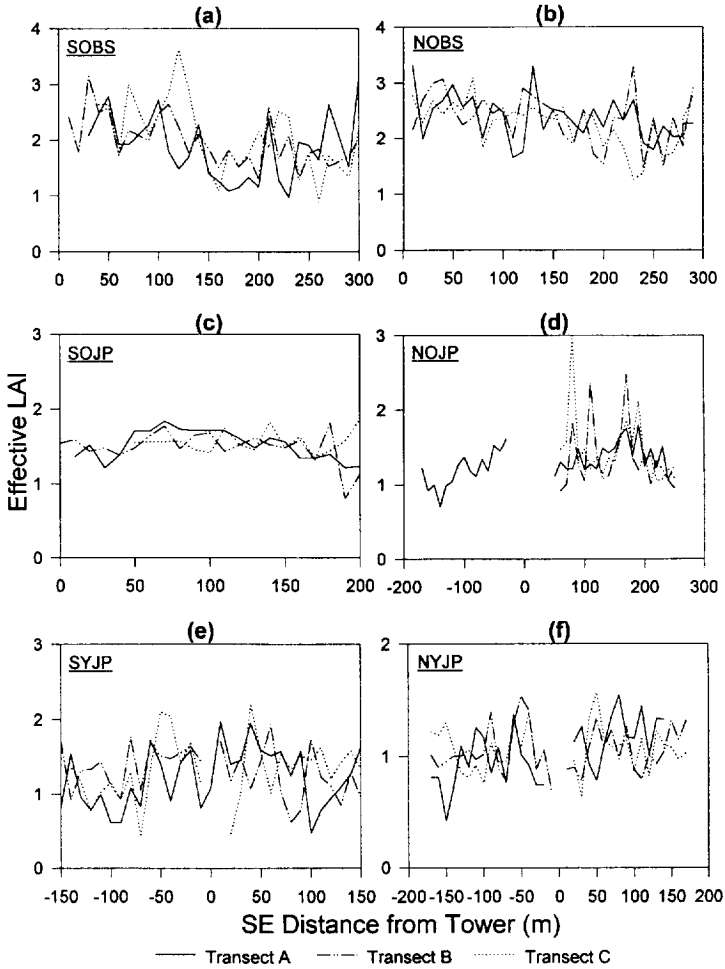

Fig. 1. Effective LAI measured in IFC'93 with the PCA on transects A, B and C for (a) SOBS, (b) NOBS, (c) SOJP, (d) NOJP, (e) SYJP and (f) NYJP. The three transects in each stand were parallel and separated by 10 m. They ran southeast (positive) or northwest (negative) from the main flux tower marked as distance 0.

presence of the understory. The predominant understory was alder (*Alnus crispa*) growing in large groups up to 5 m in diameter and 3–4 m in height. Alder grew rigorously at NOJP but much less at SOJP. Since only the overstory LAI is investigated here, the values larger than 1.8 were excluded in the mean effective LAI calculation.

Fig. 2 shows the mean effective LAI values for these six stands during the four IFCs. Each value is an average of about 90 measurements acquired on transect A, B and C, similar to those shown in Fig. 1. Black spruce and jack pine trees typically carry needles up to about three to five years old. The annual variation in leaf area index is expected to be 25% to 30% due to the needle turnover rate. However, the variations in the effective leaf area index obtained from the PCA are much smaller than the expected magnitude,

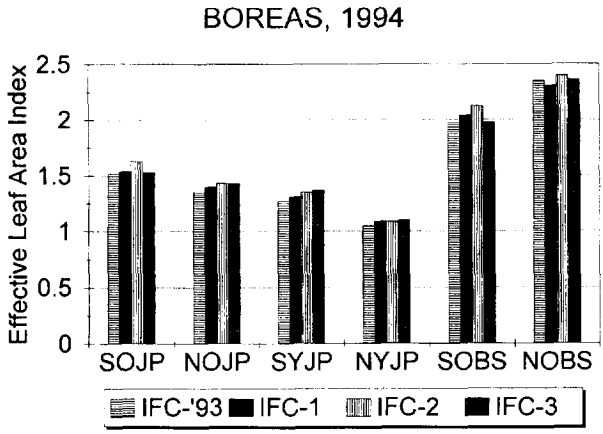

Fig. 2. A summary of the mean effective LAI measured during IFC'93, IFC-1, IFC-2 and IFC-3. These mean values are averages of 60–90 point measurements along the transects. The IFC'93 values, for example, are calculated from Fig. 1. A small seasonal variation 5–10% exists for each stand.

indicating the instrument is not sensitive to the change in LAI. The PCA derives LAI from gap fractions measured at five zenith angles. Gaps in conifer canopies exist not only within tree crowns but also largely between tree crowns. Since only the within-crown gaps decrease in size with the expansion of new needles, the total canopy gap fraction does not change in proportion to the increase in LAI. Also, new needles grow on top of old needles in the same shoots and affect only a little the gap size within the tree crowns. This small sensitivity of canopy gap fraction to the change in LAI indicates the limitation of optical instruments based on canopy gap fraction measurements.

Dates of the measurements are summarized in Table 2. Although the variation in L_e is small, the values at different times are reasonably consistent, indicating the reliability of the PCA. In most stands except for NYJP and SYJP, L_e was the largest in IFC-2 (mid-summer). In NYJP and SYJP, the IFC-3 value was the largest possibly because of the growth of the young trees. 1994 appeared to be a favourable growing year. NOBS may be the best indication of the seasonal variation pattern: the lowest value of L_e was in IFC-1 and the largest in IFC-2, and the intermediate values obtained in mid-August 1993 and early September are similar. However, in SOJP and SOBS, the IFC-1 value was not the lowest. This may be because the contribution of new growth starting in late May. Small measurement errors due to sensor calibration, sky condition variation and

Table 2
Dates of PCA measurements in 1994

	SOBS	SOJP	SYJP	NOBS	NOJP	NYJP
IFC-93	25 August	25 August	22 August	17 August	15 August	16 August
IFC-1, 94	4 June	26 May	3 June	10 June	11 June	12 June
IFC-2, 94	30 July	29 July	27 July	4 August	3 August	2 August
IFC-3, 94	11 September	10 September	10 September	2 September	7 September	5 September

reference sensor location change would add up to about 5%. Among the sources of errors, non-systematic errors may be smaller than the seasonal variability in L_e. In the SSA, conifer trees started new needle growth in late May in 1994. The PCA measurements were taken 5 to 10 days after the beginning of the new growth, and a small effect of the new growth on the effective LAI measurements is estimated to be less than 3%. In the NSA, the new growth started about 10 to 15 days later and had smaller effects on L_e than in the SSA. The oldest needles (three–five year) turned colour in late August in NSA and in early September in SSA. During IFC-3, PCA measurements were acquired in NSA and SSA after the beginning of the senescence. Small litter falls occurred before PCA measurements in NSA, but considerable needles dropped in SSA before PCA measurements, resulting in the relatively small L_e values in IFC-3 for SOJP and SOBS. In SYJP, the IFC-3 value was the highest compared with other IFC values. This is more likely due to the increase in needle area in 1994 than measurement error.

4.2. Element clumping index Ω_E

Following the method of Chen and Cihlar (1995a), visible direct solar irradiance measured along transects beneath the overstory was used to derive the element clumping index quantifying the effect of canopy architecture on LAI measured by the PCA. The element clumping index includes the effects of clumping at scales larger than the elements (shoots). Fig. 3(a)–(f) shows examples of instantaneous values of photosynthetic photon flux density (PPFD) in SOBS, SOJP, SYJP, NOBS, NOJP and NYJP, respectively. In each example, PPFD varies between a non-zero baseline to a maximum value. The baseline was measured by the diffuse sensor with a vertical shading strip. A shading factor was used to match between the two streams of data. The baseline level indicates the diffuse irradiance in the visible solar spectrum, and the maximum value is the sum of the direct PPFD above the stand and the diffuse PPFD within the stand. In SOJP and NOJP, the diffuse PPFD is fairly constant, forming a obvious straight baseline. In SOBS and NOBS, the baseline appears to be gently wavy, reaching troughs under tree crowns (where the direct radiation is small) and climbing to broad peaks under large canopy openings. In SYJP and NYJP, the diffuse irradiance is most variable because of the shorter trees. When trees are short, the sky view factor is variable, and the diffuse irradiance originating largely from the sky is also variable. In NYJP, in particular, where trees are small and short, the baseline appear to be fluctuating. The diffuse level was the lowest in SOBS and NOBS but the highest in NYJP and SYJP. In order to obtain the direct PPFD for the calculation of canopy gap size, the diffuse PPFD was subtracted from the instantaneous total PPFD.

From the trace of PPFD, one can easily tell the difference in the canopy architecture. SOJP is characterized by many large gaps (shown as large distances with maximum PPFD), indicating the distinct tree crown structure. The NYJP trace displays many small gaps with no detectable tree crown structure. Most trees in NYJP are small and the stem density is very high. Therefore gaps between tree crowns are small, and the whole canopy appears to be random. The canopy architecture difference is better demonstrated in Fig. 4(a)–(c), where the gap fraction is gradually accumulated from the largest to the smallest gaps measured over a transect, 300 m in SOBS, 190 m in SOJP and 160 m in

NYJP in these particular cases. The PCA and many other optical instruments acquire only the total accumulated gap fraction, i.e. one point on the graph. The measured gap fraction accumulation curve, $F_m(\lambda)$, illustrates the contributions of gaps of various sizes to the total gap fraction. The curve $F(\lambda)$ shows the distribution of canopy gap size if the foliage is random (Eq. (12)). The curve $F_{mr}(\lambda)$ is $F_m(\lambda)$ brought to the closest agreement with $F(\lambda)$ after removal of large gaps through the iterative procedure described in Section 2 (Theory) after Chen and Cihlar (1995a). The removed large gaps should not have existed if the foliage spatial distribution were random. In SOBS and SOJP, there were many gaps larger than 200 mm. These gaps were largely removed from the gap fraction accumulation because the probability of observing these gaps under a random canopy is very small, as shown in $F(\lambda)$. After the gap removal, the

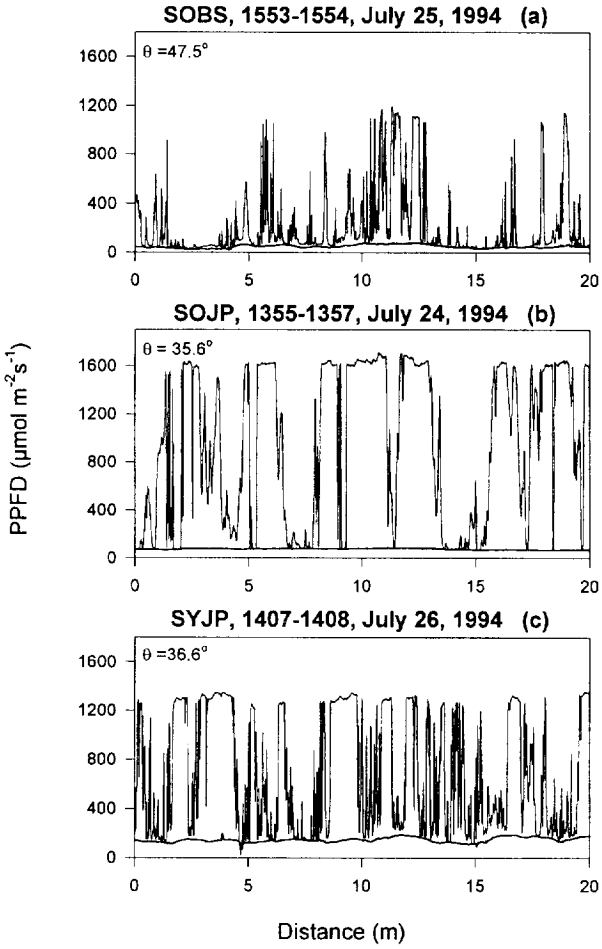

Fig. 3. Samples (20 m) of the instantaneous photosynthetically active photon flux density (PPFD) measured on transects in (a) SOBS, (b) SOJP, (c) SYJP, (d) NOBS, (e)NOJP and (f) NYJP. The bottom line represents the diffuse irradiance beneath the overstory.

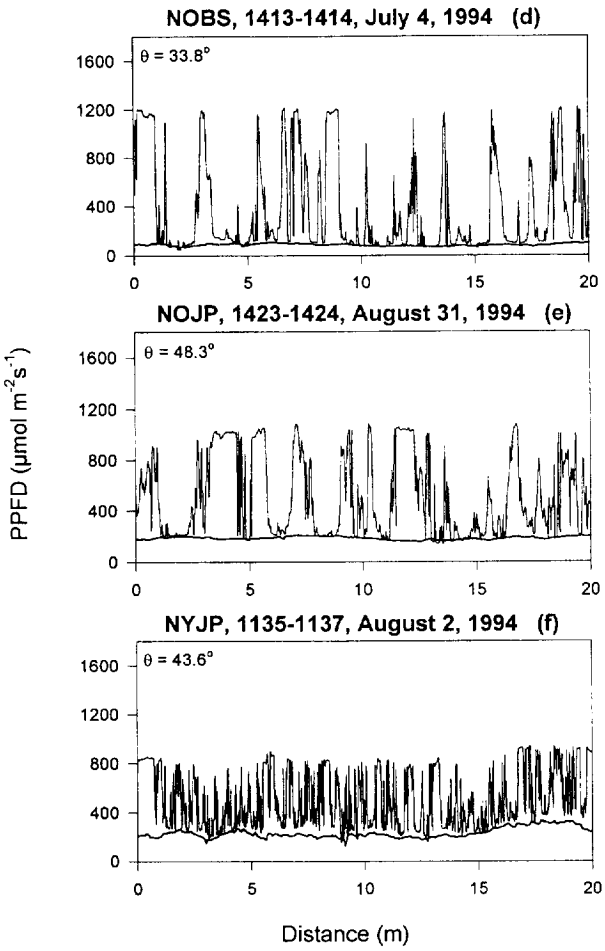

Fig. 3 (continued).

canopy is spatially compacted and becomes random. The element clumping index is calculated from the measured total gap fraction and the gap fraction for the compacted random canopy using Eq. (14). In NYJP, there were only a few gaps appearing at probabilities larger than the prediction for a random canopy. The canopy appears to be very close to the random condition.

TRAC measurements were made in each stand for IFC-1, -2 and -3 in order to investigate the possible seasonal variation in the element clumping index. The IFC-3 data are sparse Fig. 5(a)–(c) shows the variation of the element clumping index with the solar zenith angle for the three stands in the SSA. The results for the NSA stands are similar except that the NYJP result shows a small variation because the clumping index was close to unity. In all cases, the clumping index increases with increasing solar zenith angle. Two processes may have contributed to the variation. First, the canopies become

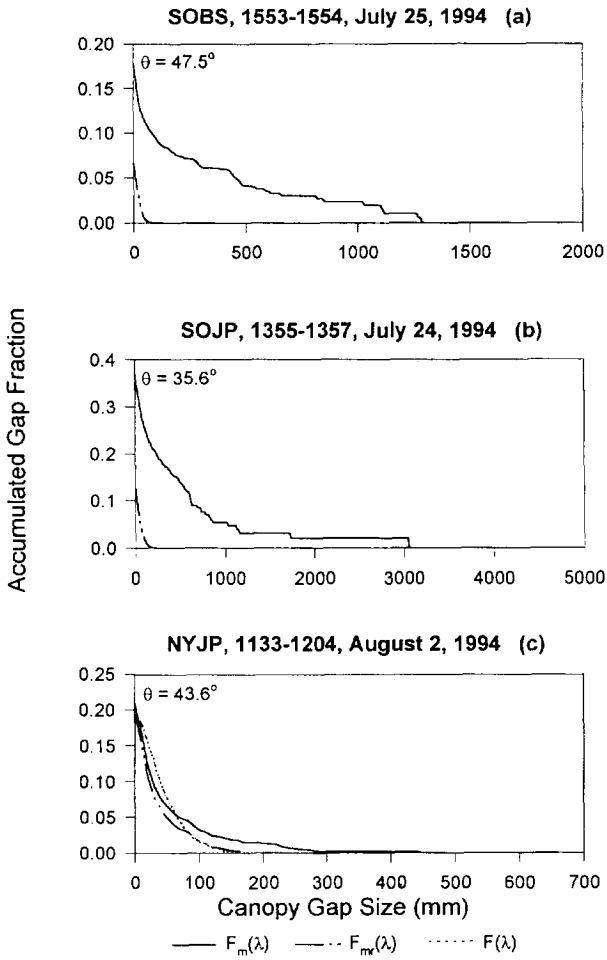

Fig. 4. Examples of canopy gap size distributions in (a) SOBS, (b) SOJP, (c) NYJP, where $F_m(\lambda)$ is the measured gap size accumulation curve, $F(\lambda)$ is the theoretical curve when the foliage spatial distribution is random, and $F_{mr}(\lambda)$ is $F_m(\lambda)$ brought to the closest agreement with $F(\lambda)$ after removal of excessively large gaps resulting from foliage clumping. In the case of SOBS and SOJP, $F_{mr}(\lambda)$ almost completely overlap with $F(\lambda)$.

less clumped (i.e. larger clumping index) as the solar zenith angle increases. Conifer tree crowns consist of branches grouped in distinct whirls at different heights. When viewed from near the vertical direction, the crowns appear solid with little gaps around the centre, but as the view zenith angle increases to near the horizontal direction, they break down into whirls or branches. Since tree crowns are the major clumping structure, their disintegration into subcomponents would make the canopies less clumped. Chen and Cihlar (1995b) found the similar increase in the element clumping index with solar zenith angle for boreal forests. Chen and Black (1992a, b) found that the clump size decreases with solar zenith angle in a Douglas-fir stand. The other process which may be

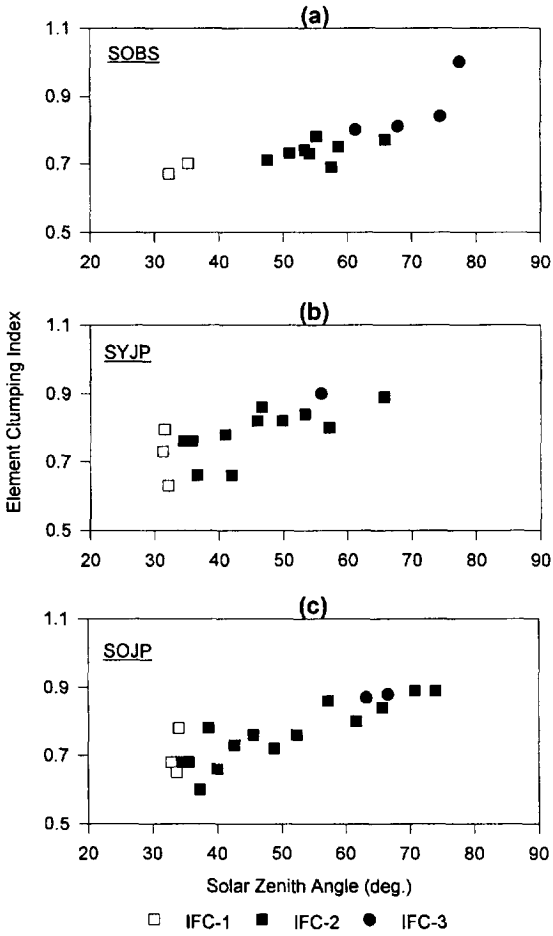

Fig. 5. Element clumping index, quantifying the effect of foliage clumping at scales larger than the shoot, as a function of the solar zenith angle for the three SSA stands.

responsible for the variation is that as the solar zenith angle increases, the penumbra effect increases and it becomes more difficult to determine small canopy gaps. Small gaps near the canopy top may disappear after multiple penumbra effects. The loss of small gaps distorts the gap size distribution and affects the gap removal process. The iteration procedure to remove the excessively large gaps is completed when a portion of the $F_{mr}(\lambda)$ curve appears under the $F(\lambda)$ curve for the random case. When the distribution at the small gap size is too much distorted, the iteration may have been prematurely completed, resulting in larger clumping indices. However, Chen and Cihlar (1995b) found that inaccuracy in determining the small gaps becomes serious only when the solar zenith angle was greater than 60°. This rule of thumb still holds in this study. We believe the second process may only have a small contribution to the variation in the clumping index with solar zenith angle. In other words the variation is real and is

unlikely due to the measurement technique. We can also look at the accuracy in another way. The random curve $F(\lambda)$ is calculated using Eq. (12). Two parameters are required to determine the distribution. One is the element width which dictates the width of the curve with respect to the canopy gap size, and the other is the element area index, L_E, which determines the accumulated gap fraction at $\lambda = 0$. The width is taking as the characteristic width of shoots which, from shoot analysis, is 30, 30, 40, 50, 60 and 60 mm for SOBS, NOBS, NYJP, NOJP, SYJP and SOJP, respectively. In the iteration process, L_E gradually increases with the decrease in $F(0)$ as large gaps are successively removed. The critical part in the gap removal process is the width of the $F_{mr}(\lambda)$ curve compared with the width of the $F(\lambda)$ curve and the accuracy in the total measured gap fraction, while the detail distribution in the $F_{mr}(\lambda)$ or $F_m(\lambda)$ only has the secondary effect. This makes the TRAC measurements of the clumping index repeatable and reliable.

As the element clumping index is not constant with the solar zenith angle, a question arises regarding how to obtain an average value for a stand. By the theorem of Miller (1967), the calculation of LAI carries the weight of $\sin\theta$ to the transmittance, i.e. larger weights are given to larger zenith angles. Theoretically, we should do the same for the clumping index since the goal of measuring this value is to improve our calculation of LAI. However, because measurements at $\theta > 60°$ are problematic, we feel it is necessary to restrict the range from 0° to 60° and apply the $\sin\theta$ weight within this range. In this case, the weighted mean value equals the value at $\theta = 39°$ assuming a linear variation of Ω_E with θ. We, therefore, extract only one clumping index value at $\theta = 39°$ for a stand. However, should Ω_E increases continuously with θ beyond 60° in reality, restricting the weighting range would result in a negative bias in the Ω_E value. Although restricting the range is a practical solution to the problem, we feel that it is also the optimum way to minimize the uncertainty due to measurement errors.

In Fig. 5(a)–(c) there is no obvious difference in Ω_E between the IFCs. This supports our argument that only the large gaps are critical in the Ω_E calculation. From IFC-1 to IFC-3, the canopies underwent new growth and senescence. The small gaps in the tree crowns varied between the IFCs, but the large gaps between the tree crowns and between whirls within crowns remained virtually unchanged. Only these large gaps are responsible for the non-random foliage spatial distribution. The small gaps between shoots within branches would have reduced as the new growth expanded in IFC-2 and increased as old needles fell in IFC-3. This small gap variation may change the gap size distribution and affects the clumping index calculation. However, the results show that the effect was very small (within the measurement error). Since the seasonal variation of Ω_E was small for all the stands investigated, only one Ω_E value at $\theta = 39°$ was determined for each stand for the calculation of LAI in the different IFCs. The values are summarized in Table 3.

Table 3
Element clumping index

SOBS	SOJP	SYJP	NOBS	NOJP	NYJP
0.70	0.71	0.71	0.71	0.82	0.95

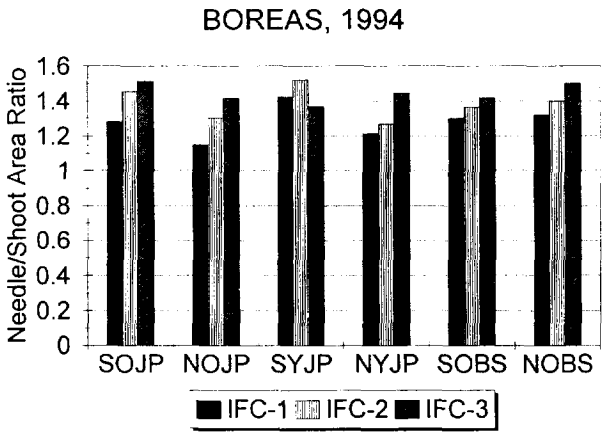

Fig. 6. A summary of needle-to-shoot area ratio, quantifying the effect of foliage clumping within the shoots, obtained from shoot samples in IFC-1, IFC-2 and IFC-3.

4.3. Needle-to-shoot area ratio

The effect of clumping within the shoots is quantified using this needle-to-shoot area ratio (γ_E). Fig. 6 shows the seasonal variation in γ_E. The value of γ_E increased from IFC-1 to IFC-2 for all the stands. In IFC-1, samples of shoots were taken about 5 to 10 days after the beginning of new growth. Although ideally the sampling should be done before the new growth, only pollen pots at the tip of shoots, in most cases, had started and their effects on the projected area was very small (less than 3%). Therefore, the IFC-1 values can be regarded to represent the condition before the new growth. In IFC-2, the new needles have extended to about 80% of the full needle length, with a small increase in the shoot projected area from which the shoot area was calculated, but there was considerable more needle area in a shoot. Hence an increase in the γ_E value is expected. From IFC-2 to IFC-3, the length of new needles further extended, but in the meantime, old needles changed colour and felt off from the canopies. The litter fall was continuous throughout the growing season but substantially increased in IFC-3 (late August and early September). Shoot samples in IFC-3 were taken during the early and middle phases of the autumn needle fall. The decrease in the foliage area is apparent in the PCA measurements (Fig. 2). We were first puzzled by the fact that the needle-to-shoot area ratio showed an increase from IFC-2 to IFC-3 rather than a decrease after the litter fall, but we provide the following explanation for this apparent contradiction. Needles felled off earlier in the summer were generally four to five years old. These needles were either distributed on stems supporting several shoots or sparsely distributed on the portion of the stem physically detached from the main collection of needles on the shoot. They were therefore not included in the shoot analysis in IFC-1 and IFC-2. The number of these old needles was considerable before the litter fall and the decrease in the L_e measured by the PCA in IFC-3 may be a result of the loss of these old needles. In selecting shoot samples, groups of needles physically close to each other were identified as shoots. They often included new growth, one to two year old needles in most cases,

Table 4
Mean needle-to-shoot area ratio and standard deviation in IFC-3 for nine tree and height classes for the six stands

	SOJP	SYJP	SOBS	NOJP	NYJP	NOBS
DT	1.86±0.36	1.64±0.05	1.61±0.12	1.64±0.23	1.64±0.06	1.75±0.06
DM	1.72±0.16	1.46±0.30	1.43±0.16	1.44±0.13	1.47±0.17	1.76±0.14
DL	1.59±0.12	1.16±0.21	1.54±0.12	1.55±0.13	1.45±0.12	1.41±0.06
MT	1.73±0.16	1.66±0.15	1.44±0.05	1.61±0.22	1.71±0.13	1.74±0.12
MM	1.68±0.20	1.34±0.07	1.35±0.08	1.40±0.30	1.44±0.05	1.64±0.06
ML	1.41±0.07	1.05±0.08	1.26±0.04	1.37±0.06	1.22±0.07	1.55±0.12
ST	1.17±0.06	1.54±0.16	1.54±0.12	1.75±0.21	1.52±0.17	1.64±0.07
SM	1.17±0.11	1.32±0.16	1.49±0.08	1.55±0.41	1.33±0.15	1.54±0.09
SL	1.32±0.32	1.10±0.10	1.37±0.10	1.38±0.16	1.23±0.16	1.47±0.12

and in some cases three year old needles were also included, especially black spruce. The older needles did not appear in distinct groups and therefore were not sampled. We believe that this sampling strategy caused the apparent problem of increasing needle-to-shoot area ratio in the early fall and is biased. Although shoots are visually distinct structures in conifer canopies (Gower and Norman, 1990; Fassnacht et al., 1994) and have been found to be well treated as the basic foliage units for radiation interception considerations (Chen and Black, 1992a, b; Chen and Cihlar, 1995a, b), it can only be considered as a treatment and an approximation to the real world. It is often difficult and sometimes arbitrary in practice to determine the shoot boundary. We didn't separate shoots by the age as done by Ross et al. (1986) because this would involved disintegrating complete shoots into unnecessary small components. Determining the clumping within shoots were the most labour intensive part of our optically-related work. It took two skilled workers about 12 intensive hours to complete the analysis of 45 shoots for a stand in one IFC. We believe the accuracy in the average γ_E for a stand is about 85% with our sampling strategy. To improve this accuracy, many more samples are required. One improvement would be to investigate the distribution pattern of the older needles and include as many old needles as possible in shoot analysis. For those which can not be included, a correction to the sampling result needs to be made according to the percentage of the older needles. This type of data were not acquired in the present study, and no such corrections were made to the results.

Table 4 summarizes the mean γ_E values and the standard deviations for IFC-3 according to the tree and height classes for all the stands. There were five samples in each class. Generally, γ_E increases with increasing height and tree size, but the increase was most pronounced with height but less with the size of trees. We believe that light availability is the major controlling factor for the variations. The variations are generally much larger than the standard deviation in each class, suggesting that separation of the classes were necessary in the sampling strategy. The mean γ_E value for a stand was taken as the arithmetic mean of the nine classes. Since in determining the height classes, the trees were separated into roughly equal foliage portions, no weighting for the height classes was therefore necessary. Larger trees carry more foliage, and therefore larger weights should be given to the larger trees in calculating the means. However, because

the differences in the γ_E values between trees were not large enough to cause significant (3%) differences in the calculated means with different weighting schemes.

4.4. Woody-to-total area ratio

Mature boreal forests have many dead branches at the lower heights. These branches and the tree trunks intercept radiation before it reaches the forest floor and affect optical measurements made near the ground. Therefore they are included in the area calculated using the combination of PCA and TRAC readings. The area of the supporting woody materials is invariant with the season, and it needs only to be determined once. Fig. 6(a)–(c) shows destructive sampling results for NOJP, SOBS, and SOJP, respectively. The sampling took place on 5, 6, and 11 and 14 September for these stands, respectively. The foliage and woody areas per tree are plotted against the square of D_{bh} assuming that the areas are proportional to the tree basal area. For all three cases, the relationships between the basal area and the foliage area or the woody area were not linear. Per unit basal area, large trees are able to support more foliage and woody areas, suggesting that dominant trees are able to use resources from the soil (water and nutrients) more efficiently for photosynthesis than the suppressed trees because they intercept more light. The allometric relationships between the half the total needle area, A_n (in m^2 per tree), half the total woody area (including branches and trunks), A_w (m^2 per tree), and half the total area (including needle, branches and trunks), A_t (m^2 per tree), with D_{bh} (m) are as follows:

SOBS:

$$A_n = 17240 \times D_{bh}^{3.0630}$$

$$A_w = 215.0 \times D_{bh}^{1.9788}$$

$$A_t = 8501 \times D_{bh}^{2.7088}$$

SOJP:

$$A_n = 820.9 \times D_{bh}^{2.2000}$$

$$A_w = 1153 \times D_{bh}^{2.7576}$$

$$A_t = 1672 \times D_{bh}^{2.3618}$$

NOJP:

$$A_n = 2224 \times D_{bh}^{2.3797}$$

$$A_w = 14490 \times D_{bh}^{3.7906}$$

$$A_t = 5741 \times D_{bh}^{2.6900}$$

Since the number of trees was small, it is estimated that these allometric relationship are subjected to relative errors of up to 30%. However, the relative error in the ratio between the woody area and total area is considerably less because much of the systematic error due to the regression is removed by taking the ratio. This scheme may be adequate for quantifying the ratio. We applied these relationships to D_{bh} of trees measured in 200 m^2 in SOJP and NOJP and 100 m^2 in SOBS to calculate the mean ratio

for the whole stand and obtained the ratio of 0.17, 0.32 and 0.28 for SOBS, SOJP and NOJP, respectively. These numbers are consistent with photographic examination which revealed considerable more dead branches in the old jack pine stands than in the old black spruce stands.

While the woody area is invariant with time, the foliage or the total area changes with season. It would seem logical to adjust the ratio for the IFCs in which the foliage area varied. However, another issue, which should be resolved before the adjustment to the ratio, is the spatial distribution pattern of the dead and live branches. Branches are located within and beneath the live tree crowns and intercept less light than when they are randomly distributed in space. Such clumping effect is largely considered in the element clumping index, which assumes that the branches and other non-green areas are clumped in a similar way as the shoots, and the error due to this assumption is estimated to be small. In mid-summer, when the foliage reached a peak, the total interception of light by the whole canopy increased only slightly as demonstrated by the PCA measurements because the new needles grew on top of the old needles and do not increase much light interception on individual shoot basis. However, the ratio of needle-to-shoot area ratio increased in IFC-2 as a result of the new growth and is used as a correction to the total area including foliage and woody materials. This simple overall correction may have introduced a positive bias because the branch area did not change in the same way as the needle area. On the other hand, the woody-to-total area ratio would have decreased from IFC-1 to IFC-2 and increased from IFC-2 to IFC-3 because of the maximum needle area growth in IFC-2. By applying a constant ratio measured in IFC-3 to convert the total area to needle area, a negative bias is introduced to IFC-2 results. These two biases are of similar magnitude and counter balance each other. For this reason, it is recommended, for the sake of simplicity and lack of detailed data, not to make adjustments to the ratio of woody-to-total area ratio measured in IFC-3.

NOBS is similar to SOBS in terms of the abundance of the dead branches, and therefore the ratio from SOBS is used for NOBS. No data were collected at NYJP and SYJP because the woody area contribution was small. From the stand density and the tree height, it is estimated that the ratio of woody to total area is 0.05 for SYJP and 0.03 for NYJP. These ratios were used to convert the total area measured optically to green foliage area.

4.5. Leaf area index

Leaf area index is calculated using Eq. (6) from the effective leaf area index (L_e), the needle-to-shoot area ratio, the element clumping index, and the woody-to-total area ratio. Fig. 7 shows the final results of leaf area index for the six stands. In SSA stands, leaf area index underwent an increase from IFC-1 to IFC-2 and a decrease from IFC-2 to IFC-3, while in NSA, it increased continuously from IFC-1 to IFC-3. The results in SSA seem reasonable because there were considerable litter falls in IFC-3, but in NSA at least the NOBS result appears to have some problems because LAI increased from IFC-2 to IFC-3 while the corresponding PCA result showed a decrease. We began IFC-3 in the NSA then proceeded to the SSA whereas the SSA stands were visited prior to the NSA stands in IFC-1 and IFC-2 (refer to Table 2 for the actual dates). In IFC-3, the

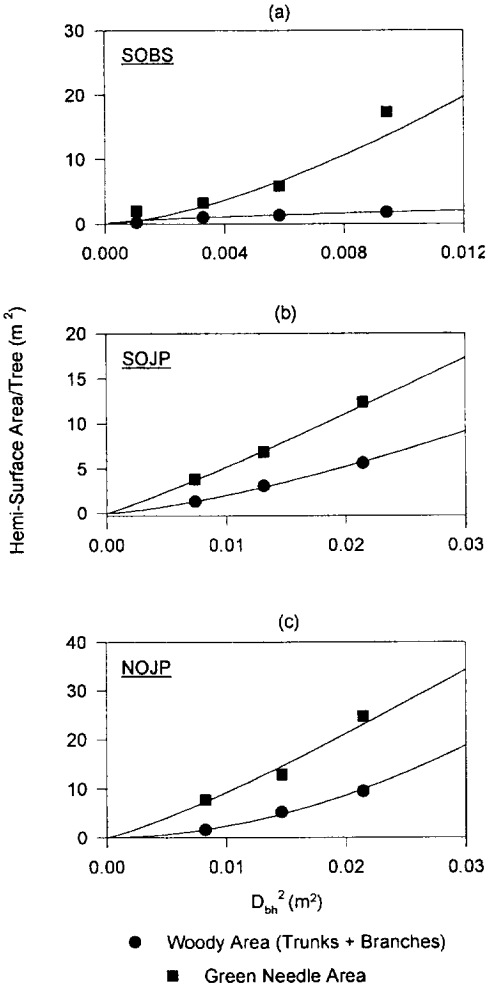

Fig. 7. Relationships of leaf area and woody area with tree trunk diameter at the breast height (D_{bh}) based on destructive sampling for (a) SOBS, (b) SOJP and (c) NOJP.

optical and shoot measurements were therefore made in the NSA stands with little needle fall. This may be part of the reason for the opposite trends in LAI from IFC-2 to IFC-3 between NSA and SSA. But we believe the error in determining the needle-to-shoot area ratio has been part of the cause of the problem. Although the relative error in the ratio for each class shown in Table 4 is small, there may be systematic positive bias due to the shoot sampling strategy which didn't not include four–five year old needles in the shoot analysis (discussed in Section 4.3). Since the effective leaf area index varied only slightly through the growing season and the element clumping index and woody-to-total area ratio were treated to be invariant with time, the seasonal variation in leaf area index is manifested largely through the needle-to-shoot area ratio. However, it appears that the

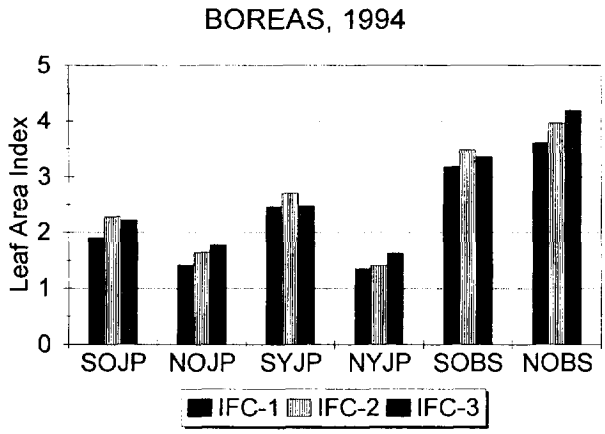

Fig. 8. Seasonal variation of leaf area index based on optical instruments and shoot sample analysis.

error in the ratio is only slightly smaller than the seasonal variability in leaf area index, resulting in uncertainties in the relative values of leaf area index estimated for the different times during the growing season. To improve the accuracy, considerably more shoot samples need to be analyzed and the sampling strategy needs to be improved.

The mean values of LAI for the stands, however, are more reliable than the seasonal variation. Forest stands in the SSA are generally denser than those in the NSA because of the latitude difference. This trend with latitude is seen in the comparisons between NOJP and SOJP and between NYJP and SYJP. The two old black spruce stands run opposite to the trend because of the local variation in the NOBS stand. SOBS represents about average conditions in SSA, while NOBS was selected with contrasting foliage conditions between the east and west sector. The east sector was much denser than the west sector in terms of foliage area and had an above-average LAI. Our transects ran from the flux tower towards to southeast direction for 300 m which was located in the denser part of the stand. The final LAI result agree with our visual impression on the stand density and the measurements of PCA (Fig. 2). An implicit requirement in using the TRAC for determining the element clumping index is that foliage clumps are penetrable by light. Black spruce trees usually have very dense tree tops with little light penetrability, and therefore the clumping effect may be larger than that measured by TRAC. If this effect is considered, the LAI values in Fig. 8 for SOBS and NOBS would be about 10% larger.

Although the destructive sampling of trees was intended to quantify the woody-to-total area ratio, the allometric equations for needle area per tree were used to calculate LAI of the three stands. The destructive LAI results (in IFC-3) are 2.4, 1.5 and 2.5 for NOJP, SOJP and SOBS, respectively. These values do not compare well with the optical results of 1.7, 2.2 and 3.3 for the same stands, respectively. The problem lies in the destructive results in several ways. First, considerable errors exist in the allometric equations. The errors not only arise from the limited sample size but also from determining the foliage area for the whole tree using ratios of shoot fresh weight to needle area (5% to 10%

error). This error may be magnified in the regression analysis using the limited number of data. Second, the optical measurements were made over transects of 170 m, 190 m and 300 m in length for NOJP, SOJP and SOBS, respectively, while the D_{bh} were sampled over only part of the transects, being 100 m, 100 m and 50 m, with a width of 20 m, for the same stands, respectively. The high stem density of these stands prevented us from acquiring the D_{bh} data for the whole transect, especially for the SOBS. The stem density variation along the transect may be considerable. Third, trees were destructively sampled about 50 m to 100 m away from the transects to preserve the stand for possible later investigations, and the allometric relationships derived from these trees may not be applicable to the trees along the transects. From our visual observation, the amount of foliage on a tree depends on not only the trunk diameter but also the surrounding foliage conditions. A tree in a relatively open area can carry considerably more foliage than a tree in the denser part of the same stand with the same diameter. In other words, allometric relationships can vary greatly depending on which area is chosen and which trees are selected, even within the same stand. Optical measurements avoid these problems and can be more accurate for obtaining average LAI values for large areas. Generally speaking, the accuracy of destructive sampling is comparable to optical measurements if allometric relationships were derived from trees in the same area and sufficient number of trees were sampled (minimum 10). However, if the relationships are applied to other areas where stem density or other environmental conditions (e.g. soil, topography and others) are different, the allometric results are expected to be much worse than the optical results. This raises an issue regarding the validation of optical LAI results. We believe that there is no easy way to validate the results for our conifer stands. A validation with an 80% accuracy would require all trees to be cut and all shoots to be clipped or all needle to be counted. This is almost impossible even if we limit ourselves to the minimum PCA measuring area which is a circle with a diameter of about 4 times the tree height. From error analysis, we believe that the optical measurements, when done carefully, can have accuracies close to or better than 80%. The total error in optical results is the sum of errors in PCA measurements (3–5%), the element clumping index (3–10%), the needle-to-shoot area ratio (5–10%), and the woody-to-total area ratio (5–12%). Hence the total error is about 15–40%. The LAI values presented in this paper are estimated to have errors of 25–35%. The best 85% accuracy can be achieved by carefully operating the PCA and TRAC, improving the shoot sampling strategy and the measurement of woody-to-total area ratio. We therefore do not recommend allometric methods for conifer stands.

5. Summary

In this paper, optical methods for quantifying seasonal variations in LAI are evaluated. It is found that the PCA is reliable in obtaining the effective LAI for the conifer stands, but the readings responded only slightly to the seasonal variation. The TRAC is also reliable in determining the effect of foliage clumping at scales larger than the shoots which is found to be invariant with season. The information of the seasonal variation is largely contained in the needle-to-shoot area ratio, which quantifies the

amount of needle area per unit shoot area measurable by optical instruments. The ratio obtained from shoot analysis in the laboratory increased from late spring (IFC-1) to middle summer (IFC-2) for all the stands as expected because of the new needle growth but further increased from mid-summer to late summer and early autumn (IFC-3) for some stands without plausible reasons. We believe the increase for the SSA stands is unrealistic because any further expansion of needles in the summer would have been overbalanced by small needle falls in the later summer and early autumn. The shoot sample analysis appears to be critical in determining the seasonal variability but also most error prone. The problem with our measurements of the ratio may be that the shoot analysis was confined to zero to three year old needles, which appeared as distinct collections of needles, whereas the older needles (four to ten years old), which were sparsely distributed, were ignored. To improve the accuracy in the measured ratio, the sampling strategy can be improved by including the older needles in the analysis. A simple three-angle scheme for measuring the shoot area provided 95–98% accuracy.

From comparisons of optical results to destructive sampling results, it is believed that optical LAI estimates (assisted with shoot samples) can generally be better than allometric LAI through laborious destructive sampling. The critical improvements in the optical measurements in this study is the use of the TRAC which removed the effect of canopy architecture on LAI measurements. The effect on average is about 30%. The combined use of the PCA and the TRAC for determining LAI in conifer stands is recommended.

Acknowledgements

This study was part of BOREAS. The author appreciates the logistic support by BOREAS operation offices in Candle Lake and Thompson. During field campaigns, Dr. John Norman of the University of Wisconsin at Madison gave useful advice and kindly provided us with a rotational light table similar to that used by Fassnacht et al. (1994) for multi-angle shoot projections. Drs. Josef Cihlar and Zhanqing Li of Canada Centre for Remote Sensing (CCRS) participated in part of the field measurements. Mr. Martin Guilbeault helped in data collection, entry, processing and archiving. Student employees Jason Nelson, Onmanda Niebergall, Debbie Miller and Darcy Delgatty contributed to intensive field and laboratory measurements. Peter White of York University was partially involved in field data collection during IFC-3. Gunar Fedosejevs of CCRS carefully reviewed the manuscript.

References

Baldocchi, D.D., Hutchison, B.A., Matt, D.R. and McMillen, R.T., 1985. Canopy radiative transfer models for spherical and known leaf inclination distribution angles: a test in an oak hickory forest. J. Appl. Ecol., 22: 539–555.

Bonan, G.B., 1993. Importance of leaf area index and forest type when estimating photosynthesis in boreal forests. Remote Sens. Environ., 43: 303–314.

Chen, J.M., Black, T.A. and Adams, R.S., 1991. Evaluation of hemispherical photography for determining plant area index and geometry of a forest stand. Agric. For. Meteorol., 56: 129–143.

Chen, J.M. and Black, T.A., 1991. Measuring leaf area index of plant canopies with branch architecture. Agric. For. Meteorol. 57: 1–12.

Chen, J.M. and Black, T.A., 1992a. Foliage area and architecture of plant canopies from sunfleck size distributions. Agric. For. Meteorol., 60: 249–266.

Chen, J.M. and Black, T.A., 1992b. Defining leaf area index for non-flat leaves. Plant Cell Environ., 15: 421–429.

Chen, J.M. and Cihlar, J., 1995a. Plant canopy gap size analysis theory for improving optical measurements of leaf area index of plant canopies. Appl. Opt., 34: 6211–6222.

Chen, J.M. and Cihlar, J., 1995b. Quantifying the effect of canopy architecture on optical measurements of leaf area index using two gap size analysis methods. IEEE Trans. Geosci. Remote Sens., 33: 777–787.

Chen, J.M. and Cihlar, J., 1996. Retreiving leaf area index of boreal conifer forests using Landsat TM images. Remote Sens. Environ., in press.

Cihlar, J., 1996. Identification of contaminated pixels in AVHRR composite images for studies of land biosphere. Remote Sens. Environ., in press.

Deblonde, G., Penner, M. and Royer, A., 1994. Measuring leaf area index with the LI-COR LAI-2000 in pine stands. Ecology, 75: 1057–1511.

Fassnacht, K., Gower, S.T., Norman, J.M. and McMurtrie, R.E., 1994. A comparison of optical and direct methods for estimating foliage surface area index in forests. Agric. For. Meteorol., 71: 183–207.

Gower, S.T. and Norman, J.M., 1990. Rapid estimation of leaf area index in forests using the LI-COR LAI-2000. Ecology, 72: 1896–1900.

Lang, A.R.G., 1991. Application of some of Cauchy's theorems to estimation of surface areas of leaves, needles and branches of plants, and light transmittance. Agric. For. Meteorol., 55: 191–212.

Leverenz, J.W. and T.M. Hinckley, 1990. Shoot structure, leaf area index and productivity of evergreen conifer stands. Tree Physiol., 6: 135–149.

Miller, J.B., 1967. A formula for average foliage density. Aust. J. Bot., 15: 141–144.

Miller, E.E. and Norman, J.M., 1971, A sunfleck theory for plant canopies. I. Lengths of sunlit segments along a transect. Agron. J., 63: 735–738.

Nilson, T., 1971. A theoretical analysis of the frequency of gaps in plant stands. Agric. Meteorol., 8: 25–38.

Norman, J.M. and Jarvis, P.G., 1974. Photosynthesis in Sitka spruce (*Picea sitchensis* (Bong.) Carr.). Part III. Measurement of canopy structure and interception of radiation. J. Appl. Ecol., 11: 375–398.

Oker-Blom, P., 1986. Photosynthetic radiation regime and canopy structure in modeled forest stands. Acta For. Fenn., 197: 1–44.

Ross, J., Kellomaki, S., Oker-Blom, P., Ross, V. and Vilikainen, L., 1986. Architecture of Scots pine crown: Phytometrical characteristics of needles and shoots. Silva Fenn., 19: 91–105.

Running, S.W. and Hunt, E.R., 1992. Generalization of a forest ecosystem process model for other biomes, BIOME-BGC, and an application of global scales. In: J.R. Ehleringer and C. Field (Editors), Scaling Process Between Leaf and Landscape Levels. Academic Press, New York.

Sellers, P.J., Mintz, Y., Sud, Y.C. and Dalcher, A., 1986. A simple biosphere model (SiB) for use within general circulation models. J. Atmos. Sci., 43: 505–531.

Smith, N.J., Chen, J.M. and Black, T.A., 1993. Effects of clumping on estimates of stand leaf area index using the LI-COR LAI-2000. Can. J. For. Res., 23: 1940–1943.

Stenberg, P., Linder, S., Smolander, H. and Flower-Ellis, J., 1994. Performance of the LAI-2000 plant canopy analyzer in estimating leaf area index of some Scots pine stands. Tree Physiol., 14: 981–995.

Spanner, M.A., Pierce, L.L., Running, S.W. and Peterson, D.L., 1990. The seasonal trends of AVHRR data of temperate coniferous forests: relationship with leaf area index. Remote Sens. Environ., 33: 97–112.